UMYU Scientifica, Vol. 3 NO. 3, September 2024, Pp 193 – 205
https://doi.org/10.56919/usci.2433.022
ISSN: 2955 – 1145 (print); 2955 – 1153 (online)
A periodical of the Faculty of Natural and Applied Sciences, UMYU, Katsina

ORIGINAL RESEARCH ARTICLE

Impact of Suction/Injection on the Non-Steady Shear-Mode Heat Mass Transfer Flow in Porous Channels

Abdullahi Sammani[1] and Hanafi Junaidu[2]

[1]School of Science and Technology, Department of Statistics, Federal Polytechnic Kaura- Namoda, Zamfara, Nigeria
[2]School of Science and Technology, Department of Statistics, Federal Polytechnic Kaura- Namoda, Zamfara, Nigeria

ARTICLE HISTORY

Received June 14, 2024
Accepted August 28, 2024
Published September 01, 2024

KEYWORDS

Suction/Injection, MHD, Unsteady, Heat transfer, Mass transfer

ABSTRACT

This study employs an implicit finite difference method to solve the transformed non-dimensional governing equations, highlighting the effects of key parameters on heat and mass transfer in porous channels. In order to demonstrate the behaviour of the flow transport phenomena, the numerical results for the velocity, temperature, and concentration profiles are graphically illustrated. Meanwhile, the skin friction, nusselt number, and sherwood number are presented graphically and discussed for a few chosen controlling thermo-physical parameters involved in the problems. It has been noted that while the concentration profile reduces with a rising value in the sequence of suction, chemical reaction, and temperature, the velocity and temperature increase due to increases in injection, thermal grashof number, variable thermal conductivity, and prandtl number. A mat lab software was used for the analysis and obtained all the results of the parameters.

INTRODUCTION

One of the methods for stopping or postponing boundary layer separation is thought to be injection or suction. Due to its numerous engineering applications, the study of heat and mass transfer via suction or injection has attracted a lot of attention. One such boundary layer control technique that aims to lower energy losses in channels is suction/injection. In the fields of aerodynamics and space sciences, the investigation of suction and injection on boundary layer control was crucial. Irranian *et al.* (2023) examined the importance of heat production and the effects of suction and injection on Maxwell fluid across a horizontal plate under radiation. Sumera et al. (2022) investigate the thermal stability of hybrid nanofluid with viscous dissipation and suction/injection applications: Dual branch framework. Majid et al. (2022) studied the impacts of chemical reaction and suction/injection on the mixed convective Williamson fluid past a penetrable porous wedge. Shojaefard et al. (2005) studied suction/injection to control fluid flow on the surface of subsonic aircraft. Ishak *et al.* (2008) analyzed the mixed convection boundary layer flow over a permeable vertical surface with prescribed wall heat flux. Abiodun and Kabir (2020) analyzed the combined effects of variable viscosity and thermal conductivity on fluid flow and thermodynamics in a vertical channel.

The study of suction/injection involves the management of fluid flow in a channel. Jha et al. (2016) looked into how injection and suction worked together to affect MHD free-convection flow in a vertical channel that was exposed to heat radiation. Uwanta and Usman (2015) investigated the magnetohydrodynamic free convective flow finite difference solutions in a Darcy-Forchheimer porous media with constant suction and variable thermal conductivity. Examined the effects of suction and injection along varying flow parameters on an unsteady MHD casson thin film flow with slip and uniform thickness over a stretching sheet. Amos *et al.* (2020) investigated the effects of chemically reacting MHD-free convective heat and mass transfer flow of dissipative casson fluid with variable viscosity and thermal conductivity.

Suction is described as the removal of fluid from a system, whereas injection is the administration of a fluid into a system, as in the case of blood transfusion. The opposing surfaces of the plates are porous, allowing fluid to enter and exit if both run simultaneously. Fluid channel suction and injection have drawn particular attention because of their crucial uses in a variety of fields, including science, engineering, petroleum drilling, and food processing sectors. Jha *et al.* (2018) looked at the effects of suction/injection on steady mixed convection flow

Correspondence: Abdullahi Sammani. School of Science and Technology, Department of Statistics, Federal Polytechnic Kaura-Namoda, Zamfara State, Nigeria. ✉ dagasammani@gmail.com.
How to cite: Abdullahi, S., & Hanafi, J. (2024). Impact of Suction/Injection on the Non-Steady Shear-Mode Heat Mass Transfer Flow in Porous Channels. *UMYU Scientifica*, 3(3), 193 – 205. https://doi.org/10.56919/usci.2433.022

through a vertical parallel micro-channel. Sarojamma *et al.* (2017) investigated the influence of thermal radiation paired with variable thermal conductivity on MHD Micropolar fluid flow over an upper surface. They also considered the fluid flow along an upper horizontal surface of a paraboloid of revolution with a porous medium.

Researchers examined a brief instance of hydromagnetic-free convection flow in the presence of suction and injection and discovered that fluid velocity drops as suction and injection increased Jha et al. (2018). The rate at which thermal energy (heat) is transferred between physical systems as a result of temperature differentials is the subject of the thermal engineering subfield of heat transfer. By lowering the drag force on the surface, suction/injection is a mechanical effect that is employed to regulate the energy losses in the boundary layer region. Uwanta and Hamza (2014) investigated how suction and injection affected the naturally occurring, unstable hydromagnetic convection flow of a viscous reactive fluid between vertical porous plates when thermal diffusion was present. Kareem and Salawu (2017) examined the effects on variable viscosity and thermal conductivity viscosity in a dissipative heat and mass transfer of an inclined magnetic field in a permeable medium past a continuously stretching surface for the power-law difference in the temperature and concentration.

Quader and Alam (2021) studied soret and dufour effects on unsteady MHD-free convective heat and mass transfer flow in the presence of Hall current and constant heat flux through a semi-infinite vertical porous plate in a rotating system with the combined soret and dufour effects. The porous plate is thought to be exposed to a continuous heat flux. Seddek and Salema (2007) studied the effects of temperature-dependent viscosity and thermal conductivity in the presence of suction and magnetic field parameters on unsteady MHD convective heat transfer across a semi-infinite vertical porous plate. Babu *et al.* (2014) used a computational technique to examine the effects of radiation and heat sources/sinks on the steady two-dimensional magnetohydrodynamic (MHD) boundary layer flow via a shrink sheet with wall mass suction.

Usman et al. (2022) investigated how mass transfer and chemical reactions in a vertical porous channel with free convective radiative flow were affected by suction and injection. Rehman *et al.* (2019) investigated the effects of heat transmission and suction/injection on unstable MHD flow over a stretchy spinning disk. This was accomplished by looking at the heat transfer over a stretchy spinning disk with mass suction/injection and unstable magneto hydro-dynamic two-dimensional boundary layer flow. Usman et al. (2017) look at how a magnetic field and chemical reaction work together to affect unsteady natural convection flow in a vertical porous channel. Lavanya and Ratmann (2014) used the effects of mass transfer and radiation on unsteady MHD natural convection flow over a vertical porous plate embedded in a porous medium in a slip flow regime with a heat source/sink to reach the analytical solution.

Bhattacharya (2014) examined the impact of a heat sink or source on mass suction-assisted shrinking sheet heat transfer and MHD flow. Hsiao (2010) investigated the radiation and heat dissipation effects of a continuous laminar boundary-layer flow of a viscous flow across a nonlinearly stretched sheet in terms of heat and mass transfer. The effect of variable viscosity and thermal conductivity on MHD-free convection flow over an isothermal vertical plate immersed in a fluid with heat conduction was studied by Sree and Alam (2021). The study of variable thermal conductivity on heat and mass transfer flow over a vertical channel with magnetic field intensity was investigated by Uwanta and Usman (2014). Despite extensive research, the combined effects of suction/injection on non-steady MHD-free convective heat mass transfer flow in porous channels remain underexplored by Parasad et al. (2020). This study aims to fill the gap of the anchor paper, which is titled The Effect of Variable Thermal Conductivity on Heat and Mass Transfer Flow over a Vertical Channel with Magnetic Field Intensity. Then, by inculcating the suction/injection parameter to investigate its effects using an implicit finite difference method and mat lab soft where will be used to obtain the results of momentum, temperature, concentration profiles, and other parameters in the equations and comparison between the result of the anchor paper and present research to show the significant of the new parameter incorporated.

MATHEMATICAL FORMULATION

The following assumptions have been made,

1. Take into account the erratic radiative flow of a viscous incompressible fluid past a vertical channel that has an intensity of magnetic field and suction or injection.
2. A transverse magnetic field of equal strength is applied to the flow direction.
3. The x-axis is moved vertically upward along the plate in the direction of the applied magnetic field, and the y-axis is normal to the plate.
4. To observe their impacts on the flow, the concentration equation is the only one where the soret is assumed. The suction is assumed in all three equations.
5. The induced magnetic field is compared to the applied magnetic field in the absence of any input electric field because it is assumed that the magnetic Reynolds number is very tiny.
6. All of the flow variables depend only on y and time (t), as the plate is infinite and the fluid motion is erratic.

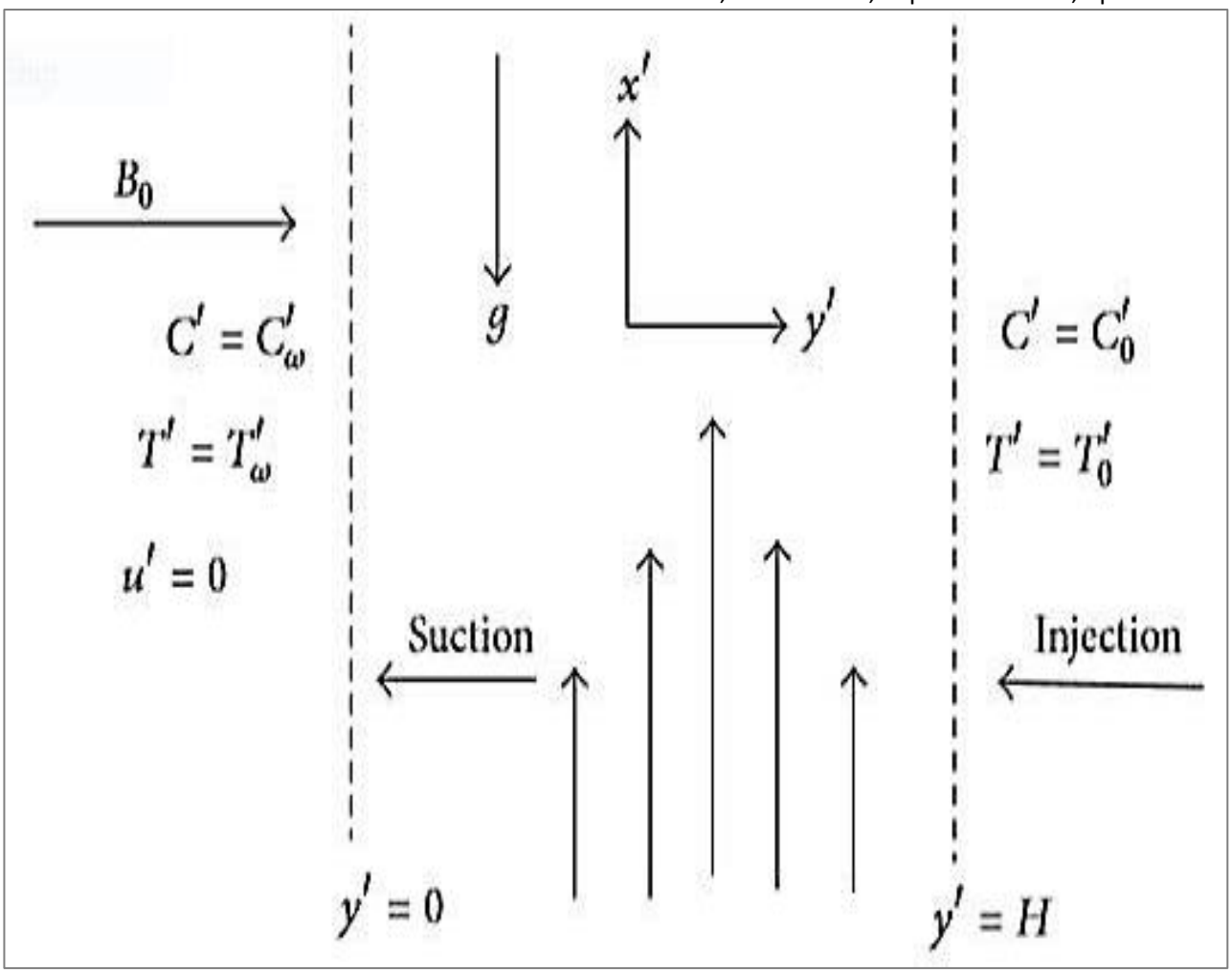

Figure 1: Coordinate System for the Physical Model of the Problem.

Solutions of the Governing Equations in Dimensionless Form Using Dimensional Quantities:

$$u = \frac{u'}{u_0}, t = \frac{t'u_0}{H^2}, y = \frac{y'}{H}, \theta = \frac{T'-T'_0}{T'_w-T'_0}$$

$$C = \frac{C'-C'_0}{C'_W-C'_0}, Pr = \frac{u_0\rho C_p}{k_0}, M = \frac{\sigma\beta_0 H^2}{\rho u_0}.$$

$$Sc = \frac{u_0}{D}, k = \frac{ku_0}{vH^2}, K_r = \frac{R^* H^2}{u_0}.$$

$$\lambda = \alpha\left(T' - T'_0\right), R = \frac{16a\sigma_0 HT'^3_0}{ku_0^2}. \quad (1)$$

$$Gr = \frac{H^2 g\beta\left(T'_w-T'_0\right)}{u_0^2}. \qquad Q = \frac{1}{\rho c\rho}\left(T' - T'_0\right)$$

$$Gc = \frac{H^2 g\beta^*\left(C'_w-C'_0\right)}{u_0^2}. \; V = \frac{v}{u_0}, Ec = \frac{1}{\rho c\rho}\left(\frac{\partial u'}{\partial y'}\right)^2$$

Then, the fully developed is governed by the following set of equations

$$\frac{\partial u'}{\partial t'} + v\frac{\partial u'}{\partial y'} = v\frac{\partial^2 u'}{\partial y^2} - \frac{\sigma\beta_0^2 u'}{\rho} - \frac{v}{k^*}u' + g\beta\left(T' - T'_0\right) + g\beta^*\left(C' - C'_0\right) \quad (2)$$

$$u = \frac{u'}{u_0} \Rightarrow uu_0 = u' \Rightarrow u_0\partial u = \partial u' \therefore \partial u' = u_0\partial u$$
$$\Rightarrow\therefore \partial^2 u' = {u_0}^2\partial^2 u$$

$$t = \frac{t'u_0}{H^2} \Rightarrow H^2 t = t'u_0 \Rightarrow H^2\partial t = u_0\partial t' \therefore \partial t' = \frac{H^2\partial t}{u_0}$$

$$y = \frac{y'}{H} \Rightarrow yH = y' \Rightarrow H\partial y = \partial y' \Rightarrow\therefore H^2\partial^2 y = \partial^2 y' \quad (3)$$

$$V = \frac{v}{u_0};$$

Substitute equation (3) into equation (2) to get the dimensionless form.

$$\left(\frac{u_0\partial u}{\frac{H^2\partial t}{u_0}}\right) + Vu_0\left(\frac{u_0\partial u}{H\partial y}\right) = v\left(\frac{u_0\partial^2 u}{H^2\partial y}\right) - \frac{u\sigma\beta_0^2 u_0}{\rho} - \frac{uvu_0}{k^*} + g\beta\left(T' - T'_0\right) + g\beta^*\left(C' - C'_0\right) \quad (4)$$

Multiply through by $\frac{H^2}{u_0^2}$;

$$\left(\frac{H^2}{u_0^2}\times\frac{u_0^2}{H^2}\right)\frac{\partial u}{\partial t}+V\left(\frac{H^2}{u_0^2}\times\frac{u_0^2}{H^2}\right)\frac{\partial u}{\partial y}=v\left(\frac{H^2}{u_0^2}\times\frac{u_0^2}{H^2}\right)\frac{\partial^2 u}{\partial y^2}-\frac{u\sigma\beta_0^2u_0}{\rho}\times\frac{H^2}{u_0^2}-\frac{uvu_0}{k^*}\times\frac{H^2}{u_0^2}+\frac{H^2}{u_0^2}\times g\beta\left(T'-T_0'\right)+\frac{H^2}{u_0^2}\times g\beta^*\left(C'-C_0'\right) \quad (5)$$

$$\frac{\partial u}{\partial t}+V\left(\frac{1}{H}\right)\frac{\partial u}{\partial y}=v\frac{\partial^2 u}{\partial y^2}-\frac{u\sigma\beta_0^2u_0H^2}{\rho u_0}-\frac{uvu_0H^2}{k^*u_0}+\frac{H^2}{u_0^2}g\beta\left(T'-T_0'\right)+\frac{H^2}{u_0^2}g\beta^*\left(C'-C_0'\right) \quad (6)$$

where; $\frac{1}{H}=1, \frac{\sigma\beta_0^2u_0H^2}{\rho u_0}=M, \quad \frac{vH^2}{u_0k^*}=\frac{u_0k^*}{vH^2}=\frac{1}{k'}$, $\frac{H^2}{u_0^2}g\beta\left(T'-T_0'\right)=Gr,$

$$\frac{H^2}{u_0^2}g\beta^*\left(C'-C_0'\right)=Gc. \quad (7)$$

$$\therefore\frac{\partial u}{\partial t}+V\frac{\partial u}{\partial y}=v\frac{\partial^2 u}{\partial y^2}-Mu-\frac{1}{k^*}u+Gr\theta+GcC \quad (8)$$

$$\frac{\partial T'}{\partial t'}+v\frac{\partial T'}{\partial y'}=\frac{k_0}{\rho Cp}\frac{\partial}{\partial y'}\left[1+\alpha\left(T'-T_0'\right)\frac{\partial T'}{\partial y'}\right]-\frac{1}{\rho Cp}\frac{\partial q_r}{\partial y'} \quad (9)$$

$$\partial T=\left(T'-T_0'\right)\partial\theta, \partial y=\frac{H}{u_0}\partial y, \quad \partial t'=\frac{H}{u_0^2}\partial t, \frac{1}{\rho C_p}\frac{\partial q_r}{\partial y'}=\frac{16a_R\sigma_0^*T_0^3\left(T'-T_0'\right)\theta}{\rho C_p}, \lambda=\alpha\left(T'-T_0'\right) \quad (10)$$

Substitute equation (10) into equation (9) to get the dimensionless

$$\left(\frac{\left(T'-T_0'\right)}{\frac{H}{u_0}}\right)\frac{\partial\theta}{\partial t}+v\left(\frac{T'-T_0'}{\frac{H}{u_0}}\right)\frac{\partial\theta}{\partial y}=\frac{k_0\left(T'-T_0'\right)}{\rho C_p}\frac{\partial}{\partial y}\left[\alpha\left(T'-T_0'\right)\theta\right]\frac{\partial\theta}{\partial y}+\frac{k_0\left(T'-T_0'\right)}{\rho C_p}(1+\lambda\theta)\frac{\partial^2\theta}{\partial y^2}-\frac{16a_R\sigma_0^*T_0^3\left(T'-T_0'\right)\theta}{\rho C_p} \quad (11)$$

$$\left(\frac{u_0^2\left(T'-T_0'\right)}{H}\right)\frac{\partial\theta}{\partial t}+vu_0\left(\frac{T'-T_0'}{H}\right)\frac{\partial\theta}{\partial y}=\frac{k_0\left(T'-T_0'\right)}{\rho C_p}\frac{\partial}{\partial y}\left[\alpha\left(T'-T_0'\right)\theta\right]\frac{\partial\theta}{\partial y}+\frac{k_0\left(T'-T_0'\right)}{\rho C_p}(1+\lambda\theta)\frac{\partial^2\theta}{\partial y^2}-\frac{16a_R\sigma_0^*T_0^3\left(T'-T_0'\right)\theta}{\rho C_p} \quad (12)$$

Multiply through by $\frac{H}{u_0^2\left(T'-T_0'\right)}$,

$$\frac{\partial\theta}{\partial t}+V\frac{\partial\theta}{\partial y}=\frac{\lambda Hk_0}{u_0^2\rho C_p}\left(\frac{\partial\theta}{\partial y}\right)^2+\frac{Hk_0}{u_0^2\rho C_p}(1+\lambda\theta)\frac{\partial^2\theta}{\partial y^2}-\frac{16a_R\sigma_0^*T_0^3H\theta}{u_0^2\rho C_p} \quad (13)$$

where, $Pr=\frac{u_0\rho C_p}{Hk_0}, V=\frac{v}{u_0}, R=\frac{16a_R\sigma_0^*T_0^3H}{u_0^2\rho C_p}$ (14)

$$\therefore\frac{\partial\theta}{\partial t}+V\frac{\partial\theta}{\partial y}=\frac{\lambda}{Pr\left(\frac{\partial\theta}{\partial y}\right)^2\frac{1}{Pr(1+\lambda\theta)\frac{\partial^2\theta}{\partial y^2}}} \quad (15)$$

$$\frac{\partial c'}{\partial t'}+v\frac{\partial c'}{\partial y'}=D\frac{\partial^2 c'}{\partial y^2}-R^*\left(C'-C_0'\right) \quad (16)$$

$$C=\frac{\left(C'-C_0'\right)}{\left(C_w'-C_0'\right)}\Rightarrow\left(C_w'-C_0'\right)C=\left(C'-C_0'\right)\Rightarrow\partial C=\frac{\left(C'-C_0'\right)}{\left(C_w'-C_0'\right)}\Rightarrow\partial^2C=\frac{\left(C'-C_0'\right)}{\left(C_w'-C_0'\right)}$$

$$V=\frac{v}{u_0}, Sc=\frac{u_0}{D}\Rightarrow DSc=u_0\Rightarrow\therefore D=\frac{u_0}{Sc}, Kr=\frac{R^*H^2}{u_0}\Rightarrow u_0Kr=R^*H^2\Rightarrow\therefore R^*=\frac{u_0Kr}{H^2}$$

$$t=\frac{t'u_0}{H^2}\Rightarrow tH^2=u_0t'\Rightarrow H^2\partial t=u_0\partial t'\Rightarrow\therefore\partial t=\frac{u_0}{H^2}\partial t', y=\frac{y'}{H}\Rightarrow Hy=y'\Rightarrow H\partial y=\partial y' \quad (17)$$

Substitute equation (17) into equation (16) to get a dimensionless form:

$$\left(\frac{\left(C'-C_0'\right)}{\left(C_w'-C_0'\right)}\frac{u_0}{H^2}\right)\frac{\partial C}{\partial t}+v\left(\frac{\left(C'-C_0'\right)}{\left(C_w'-C_0'\right)}\frac{u_0}{H}\right)\frac{\partial C}{\partial y}=\frac{1}{Sc}\left(\frac{\left(C'-C_0'\right)}{\left(C_w'-C_0'\right)}\frac{u_0}{H^2}\right)\frac{\partial^2C}{\partial y^2}-\frac{u_0Kr}{H^2}\left(C'-C_0'\right) \quad (18)$$

Multiply through by $\left(\frac{\left(C_w'-C_0'\right)}{\left(C'-C_0'\right)}\right)\frac{H^2}{u_0}$

$$\left(\frac{\left(C'-C_0'\right)}{\left(C_w'-C_0'\right)}\frac{u_0}{H^2}\times\left(\frac{\left(C_w'-C_0'\right)}{\left(C'-C_0'\right)}\right)\frac{H^2}{u_0}\right)\frac{\partial C}{\partial t}+v\left(\frac{\left(C'-C_0'\right)}{\left(C_w'-C_0'\right)}\frac{u_0}{H}\times\left(\frac{\left(C_w'-C_0'\right)}{\left(C'-C_0'\right)}\right)\frac{H^2}{u_0}\right)\frac{\partial C}{\partial y}=\frac{1}{Sc}\left(\frac{\left(C'-C_0'\right)}{\left(C_w'-C_0'\right)}\frac{u_0}{H^2}\times\left(\frac{\left(C_w'-C_0'\right)}{\left(C'-C_0'\right)}\right)\frac{H^2}{u_0}\right)\frac{\partial^2C}{\partial y^2}-\frac{u_0Kr}{H^2}\times\left(\frac{\left(C_w'-C_0'\right)}{\left(C'-C_0'\right)}\right)\frac{H^2}{u_0}\left(C'-C_0'\right) \quad (19)$$

$$\frac{\partial C}{\partial t}+v\left(\frac{1}{H}\right)\frac{\partial C}{\partial y}=\frac{1}{Sc}\frac{\partial^2C}{\partial y^2}-Kr\left(C_w'-C_0'\right) \quad (20)$$

where, $V=\frac{v}{H}, C=\left(C_w'-C_0'\right)$ (21)

$$\therefore\frac{\partial C}{\partial t}+V\frac{\partial C}{\partial y}=\frac{1}{Sc}\frac{\partial^2C}{\partial y^2}-KrC \quad (22)$$

With corresponding boundary conditions,

$$t\le0, u=0, \theta=C=0 for all y$$
$$t>0, u=0, \theta=1, C=1 at y=0$$
$$u=0, \theta=0, C=0 at y=1 \quad (23)$$

For this kind of boundary layer flow, the skin-friction coefficient, Nusselt number, and Sherwood number are crucial physical parameters that can be obtained in non-dimensional form by:

$$C_f = \left(\frac{\partial u}{\partial y}\right)_{y=0}, Nu = -\left(\frac{\partial \theta}{\partial y}\right)_{y=0}, Sh = \left(\frac{\partial C}{\partial y}\right)_{y=0} \quad (24)$$

The non-dimensional quantities are reduced to the following:

$$\text{(i)}\ \ \frac{\partial u}{\partial t} + V\frac{\partial u}{\partial y} = \frac{\partial^2 u}{\partial y^2} - \left(m + \frac{1}{k}\right)u + Gr\theta + GcC \quad (25)$$

$$\text{(ii)}\ Pr\frac{\partial \theta}{\partial t} + Pr\,V\frac{\partial \theta}{\partial y} = (1+\lambda\theta)\frac{\partial^2 \theta}{\partial y^2} + \lambda\left(\frac{\partial \theta}{\partial y}\right)^2 - R\theta \quad (26)$$

$$\text{(iii)}\ Sc\frac{\partial C}{\partial t} + ScV\frac{\partial C}{\partial y} = \frac{\partial^2 C}{\partial y^2} - ScKrC \quad (27)$$

The initial and boundary conditions in non-dimensional quantities are:

$$t \le 0, u = 0, \theta = C = 0 for all y$$
$$t > 0, u = 0, \theta = 1, C = 1 at y = 0$$
$$u = 0, \theta = 0, C = 0 at y = 1 \quad (28)$$

NUMERICAL SOLUTION PROCEDURE

An implicit finite difference method has been used to solve the unstable non-linear coupled partial differential equations (25) - (27) with the agreed initial and boundary conditions (28). Using the approach, the following finite difference equations are equal to equations (25)–(27):

$$\frac{u_i^{j+1} - u_i^j}{\Delta t} + V\left(\frac{u_{i+1}^j - u_i^j}{\Delta y}\right) = \frac{1}{(\Delta y)^2}\left(u_{i+1}^{j+1} - 2u_i^{j+1} + u_{i-1}^{j+1}\right) - Mu_i^j - \frac{1}{k}u_i^j + Gr\theta_i^j + GcC_i^j \quad (29)$$

$$\frac{U_i^{j+1} - U_i^j}{\Delta t} + V\frac{U_{i+1}^j - U_i^j}{\Delta y} = \frac{U_{i+1}^{j+1} - 2U_i^{j+1} + U_{i-1}^{j+1}}{(\Delta y)^2} - \left(m + \frac{1}{k}\right)U_i^j + Gr\theta_i^j + GcC_i^j$$

Multiply through by Δt

$$\Delta t \times \frac{U_i^{j+1} - U_i^j}{\Delta t} + \Delta t \times V\frac{U_{i+1}^j - U_i^j}{\Delta y} = \Delta t \times \frac{U_{i+1}^{j+1} - 2U_i^{j+1} + U_{i-1}^{j+1}}{(\Delta y)^2} - \Delta t \times \left(m + \frac{1}{k}\right)U_i^j + \Delta t \times Gr\theta_i^j + \Delta t \times GcC_i^j \quad (30)$$

$$\left(U_i^{j+1} - U_i^j\right) + V\frac{\Delta t}{\Delta y}\left(U_{i+1}^j - U_i^j\right) = \frac{\Delta t}{(\Delta y)^2}\left(U_i^{j+1} - 2U_i^{j+1} + U_i^j\right) - \Delta t\left(m + \frac{1}{k}\right)U_i^j + \Delta t Gr\theta_i^j + \Delta t GcC_i^j \quad (31)$$

Where, $r_1 = \frac{\Delta t}{(\Delta y)^2}, r_2 = \frac{\Delta t V}{(\Delta y)} p = m + \frac{1}{k}$

$$r_3 = 1 + 2r_1, r_4 = 1 + r_2 - P\Delta t, r_5 = \Delta t Gr\theta_i^j \quad r_6 = \Delta t GcC_i^j \quad (32)$$

Substitute equation (32) into equation (31).

$$\therefore -r_1 U_{i-1}^{j+1} + r_3 U_I^{j+1} + r_1 U_{i+1}^{j+1} = r_4 U_i^j - r_2 U_{1+1}^j + r_5\theta_i^j + r_6 C_i^j \quad (33)$$

$$\left(\frac{\theta_i^{j+1} - \theta_i^j}{\Delta t}\right) + V\left(\frac{\theta_{i+1}^j - \theta_i^j}{\Delta y}\right) = \frac{\left(1+\lambda\theta_i^j\right)}{Pr(\Delta y)^2}\left(\theta_{i+1}^{j+1} - 2\theta_i^{j+1} + \theta_{i-1}^{j+1}\right) + \frac{\lambda}{Pr\left(\theta_{i+1}^j - \theta_i^j\right)^2 \frac{R}{Pr_i^j}} \quad (34)$$

Multiply through by Δt

$$\Delta t \times \left(\frac{\theta_i^{j+1} - \theta_i^j}{\Delta t}\right) + \Delta t \times V\left(\frac{\theta_{i+1}^j - \theta_i^j}{\Delta y}\right) = \frac{\Delta t \times \left(1+\lambda\theta_i^j\right)}{Pr(\Delta y)^2}\left(\theta_{i+1}^{j+1} - 2\theta_i^{j+1} + \theta_{i-1}^{j+1}\right) + \frac{\lambda}{Pr\frac{\Delta t}{(\Delta y)^2}\left(\theta_{i+1}^j - \theta_i^j\right)^2 \frac{R}{Pr_i^j}} \quad (35)$$

$$\left(\theta_i^{j+1} - \theta_i^j\right) + V\frac{\Delta t}{\Delta y}\left(\theta_{i+1}^j - \theta_i^j\right) = \left[\frac{1+\lambda\theta_i^j}{Pr}[]\frac{\Delta t}{(\Delta y)^2}\left(\theta_{i+1}^{j+1} - 2\theta_i^{j+1} + \theta_{i-1}^{j+1}\right)\frac{\lambda}{Pr\frac{\Delta t}{(\Delta y)^2}\left(\theta_{i+1}^j - \theta_i^j\right)^2 \frac{R}{Pr_i^j}}\right] \quad (36)$$

Where, $r_1 = \frac{\Delta t}{(\Delta y)^2}; P = \left[\frac{1+\lambda\theta_i^j}{Pr}[]_2\frac{V\Delta t}{\Delta y}{}_3\frac{\lambda}{Pr\frac{\Delta t}{(\Delta y)^2}{}_4\frac{R}{Pr}}\right]$ (37)

Substitute equation (37) into equation (36).

$$\therefore -Pr_1\,\theta_{i+1}^{j+1} + (1 + 2\,Pr_1\,\square)\theta_i^{j+1} - Pr_1\,\theta_{i-1}^{j+1} = (1 - r_2 - r_4)\theta_i^j - r_2\theta_{i+1}^j + r_3\left(\theta_{i+1}^j - \theta_i^j\right)^2 \quad (38)$$

$$Sc\left(\frac{C_i^{j+1} - C_i^j}{\Delta t}\right) + ScV\left(\frac{C_{i+1}^j - C_i^j}{\Delta y}\right) = \frac{1}{(\Delta y)^2}\left(C_{i+1}^{j+1} - 2C_i^{j+1} + C_i^{j+1}\right) - ScKrC_i^j \quad (39)$$

Multiply through by Δt

$$\Delta t \times Sc\left(\frac{C_i^{j+1} - C_i^j}{\Delta t}\right) + \Delta t \times ScV\left(\frac{C_{i+1}^j - C_i^j}{\Delta y}\right) = \frac{\Delta t}{(\Delta y)^2}\left(C_{i+1}^{j+1} - 2C_i^{j+1} + C_i^{j+1}\right) - \Delta t \times ScKrC_i^j \quad (40)$$

$$Sc\left(C_i^{j+1} - C_i^j\right) + \Delta t ScV\left(\frac{C_{i+1}^j - C_i^j}{\Delta y}\right) = \frac{\Delta t}{(\Delta y)^2}\left(C_{i+1}^{j+1} - 2C_i^{j+1} + C_i^{j+1}\right) - \Delta t ScKrC_i^j \quad (41)$$

Where, $r_1 = \frac{\Delta t}{(\Delta y)^2}, r_{13} = \frac{\Delta t ScV}{\Delta y}, r_{14} = (Sc + 2r_1), r_{15} = (Sc + r_{13} - \Delta t Kr)$ (42)

Substitute equation (42) into equation (41).

$$\therefore -r_1 C_{i-1}^{j+1} + r_{14} C_i^{j+1} - r_1 C_{i+1}^{j+1} = r_{15} C_i^j - r_{13} C_{i+1}^j \quad (43)$$

The initial and boundary conditions may be expressed as:

$$\left.\begin{array}{l} u_{i,j} = 0, \theta_{i,j} = 0, C_{i,j} = 0 \\ u_{0,j} = 0, \theta_{0,j} = 1, C_{0,j} = 1 \\ u_{H,j} = 0, \theta_{H,j} = 0, C_{H,j} = 0 \end{array}\right\} \quad (44)$$

The numerical solutions are as follows:

$$-r_1 U_{i-1}^{j+1} + r_3 U_I^{j+1} + r_1 U_{i+1}^{j+1} = r_4 U_i^j - r_2 U_{1+1}^j + r_5 \theta_i^j + r_6 C_i^j \quad (45)$$

$$-Pr_1\, \theta_{i+1}^{j+1} + (1 + 2\,Pr_1 \boxed{})\theta_i^{j+1} - Pr_1\, \theta_{i-1}^{j+1} = (1 - r_2 - r_4)\theta_i^j - r_2 \theta_{i+1}^j + r_3 \left(\theta_{i+1}^j - \theta_i^j\right)^2 \quad (46)$$

$$-r_1 C_{i-1}^{j+1} + r_{14} C_i^{j+1} - r_1 C_{i+1}^{j+1} = r_{15} C_i^j - r_{13} C_{i+1}^j \quad (47)$$

The index i represents space y, while the index j represents time t. The mesh size along the y-direction is represented by and the time t-direction by, respectively. The Thomas algorithm is utilized to solve the tri-diagonal system of equations that are established at each internal nodal point on a specific n-level by the finite difference equations (45) - (47).

Equations (46) and (47) are used to compute the temperature and concentration profiles for each time step. The obtained values are then utilized to generate the velocity profile at the end of the time steps, which is derived from equation (45). This process is repeated until the stable state is achieved. It is presumed that the steady-state solution to the convergence criteria for system stability has been attained.

Equations (2-8) show the solution of the velocity equation from non-dimensional form to dimensionless form using dimensional quantities from equation (1), while equations (9-15) also show the solution of the temperature from non-dimensional form to dimensionless form using dimensional quantities from equation (1) and lastly concentration equations was also simplified from non-dimensional form to dimensionless form from equations (16-22) using same dimensional quantities of equation (1).

The numerical solution of the dimensionless form of the velocity equation was evaluated from equations (29-33), while the temperature equation was also from equations (34-38), and the concentration equation was from equations (39-43).

RESULTS AND DISCUSSION

This section contains the fluid flow analysis. The major parameters, including the chemical reaction (M), dimensionless time (Gr), temperature Grashof number (G_C), Solutal Grashof number (K), Radiation parameter (R), Prandtl number (P_r), Schmidt number (S_C), Magnetic field (M), and Porous parameter are all computed numerically for a range of values. The impact of these controlling factors on the transient velocity, temperature, and concentration profiles is the main focus of this investigation.

The default values of the thermo physical parameters are specified as follows:

$$Gr = 5, Gc = 5, M = 2, Pr = 0.71, k = 0.5$$
$$R = 5, \lambda = 0.5, Kr = 1, Sc = 0.60$$

COMPARISON FIGURES ON VELOCITY PROFILES WITH DIFFERENT VALUES OF GRASHOF NUMBER *(Gr).*

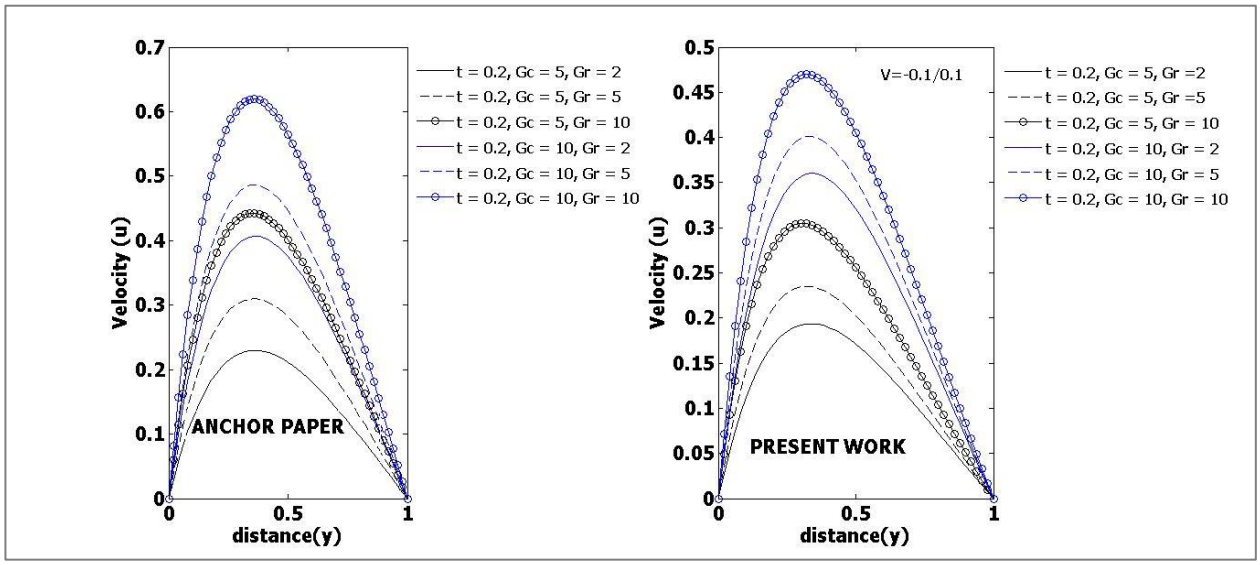

Figures 2 & 3: Velocity profiles showing the effects of grashof number *(Gr)* on the present work compared to the work of Uwanta & Usman (2014)

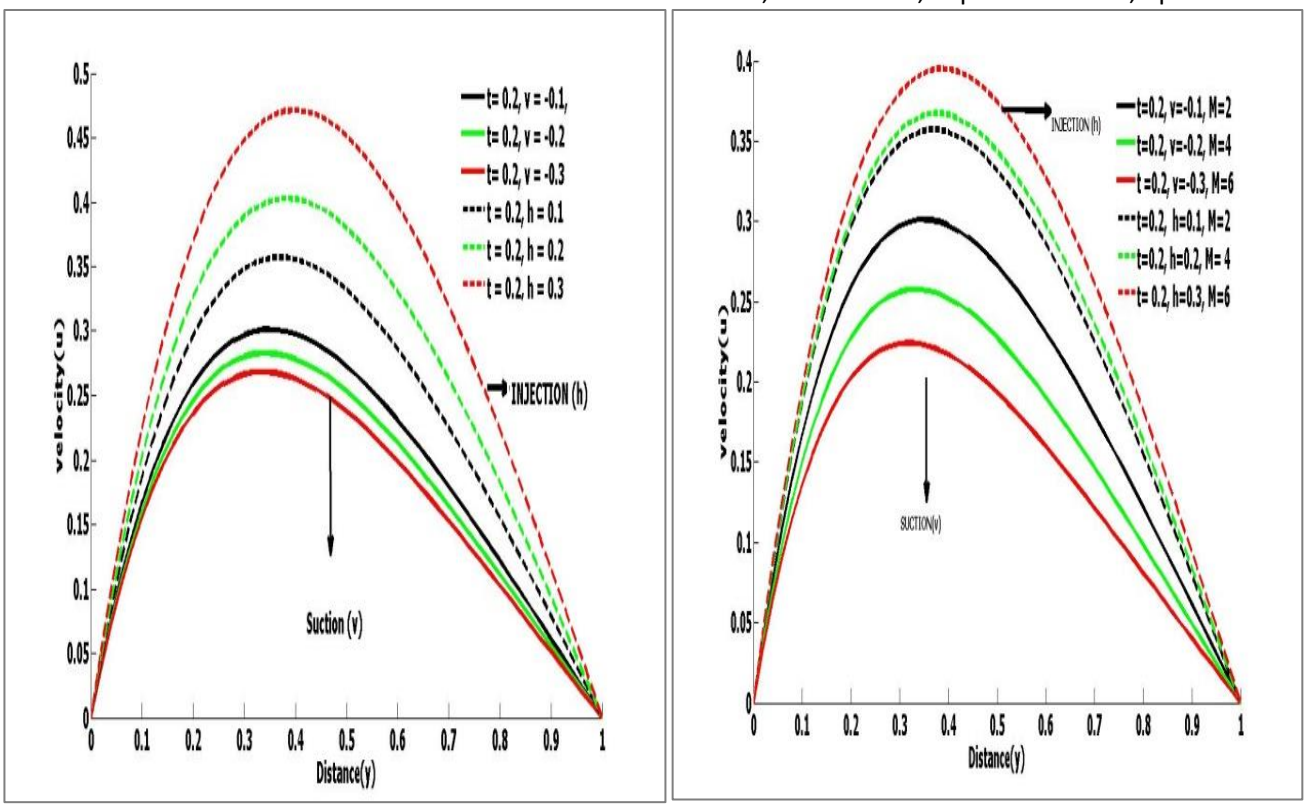

Figures 4 & 5: Velocity profile for different values of Injection or Suction (*V*) and Magnetic Field (M).

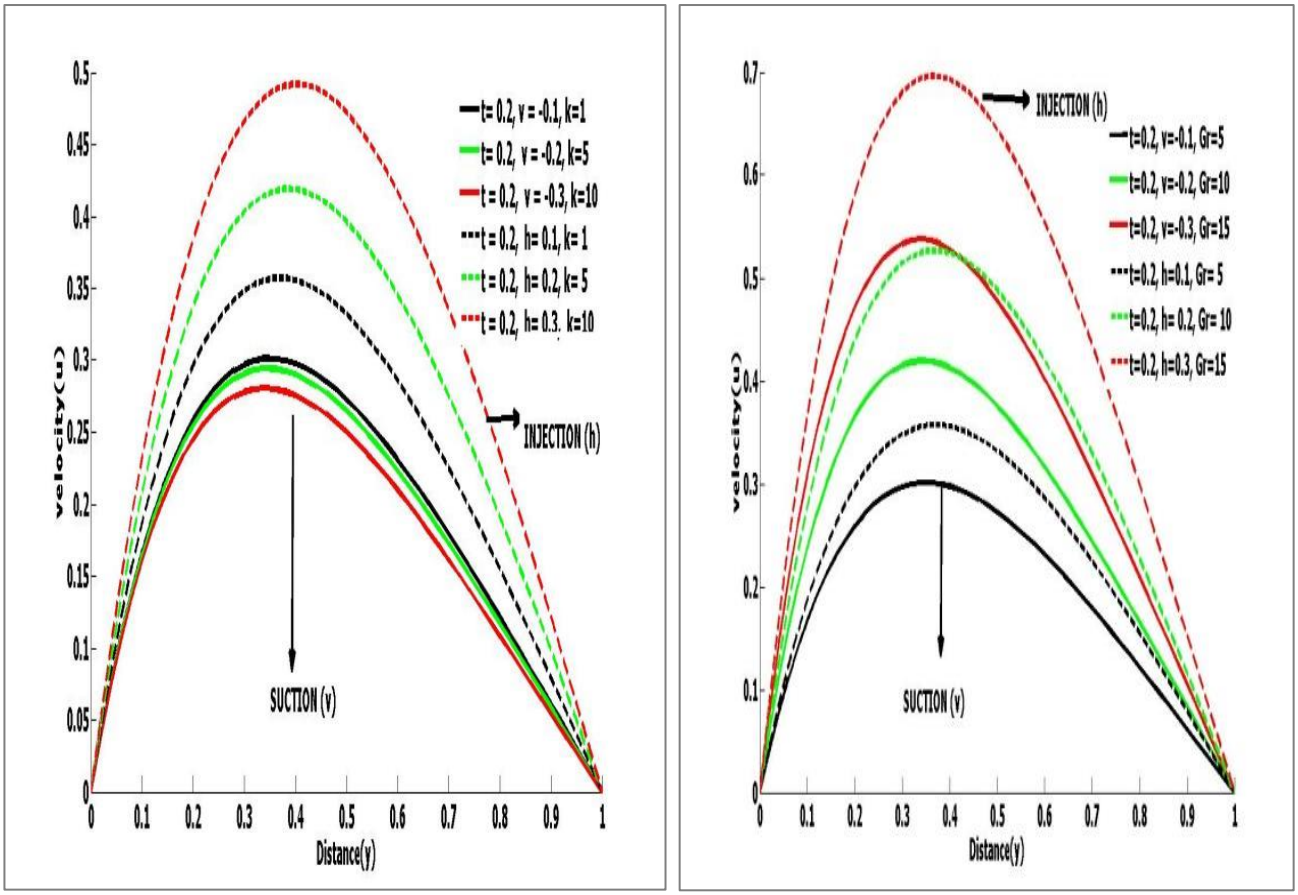

Figures 6 & 7: Velocity profile for different values of Porous (k) thermal Grashof numbers (*Gr*).

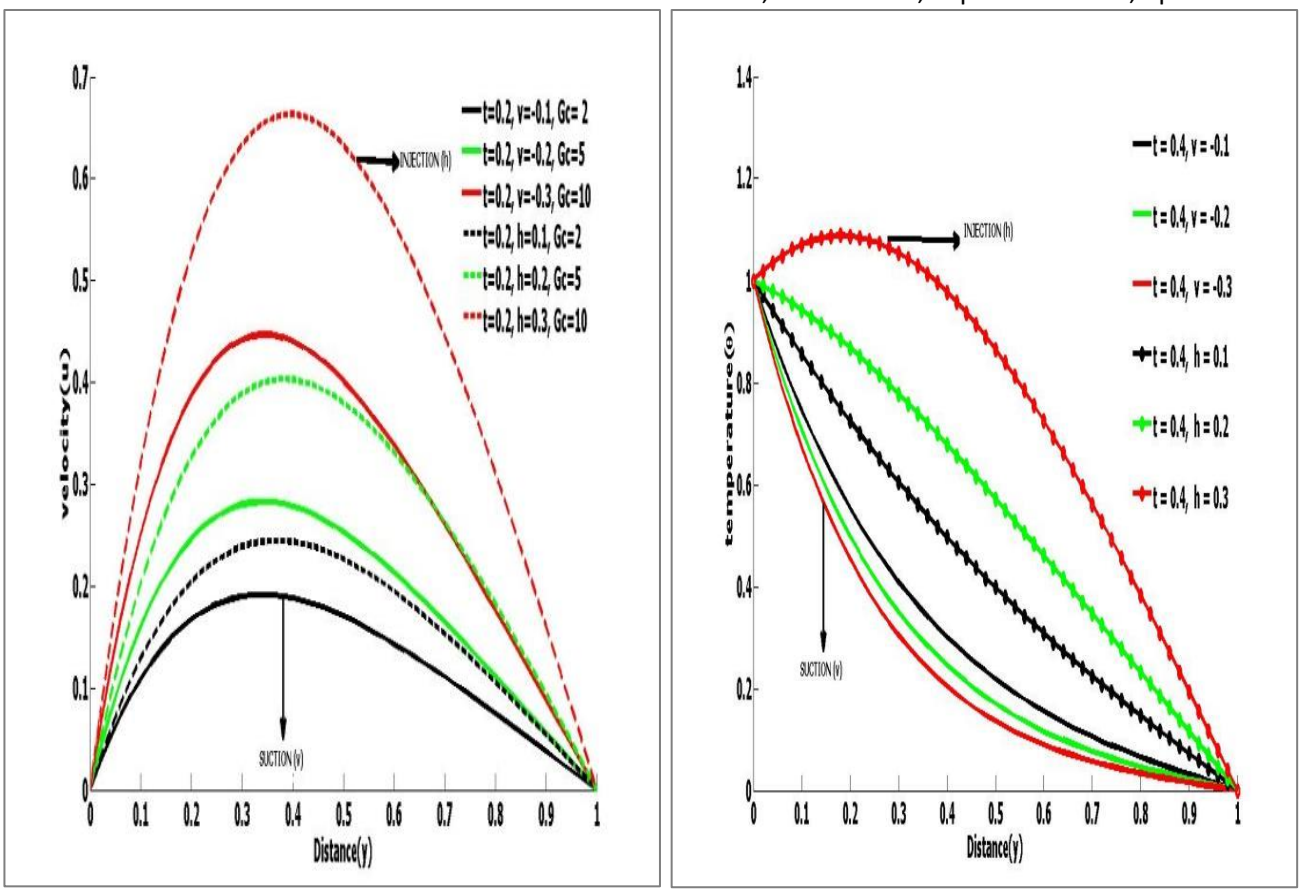

Figsures 8 & 9: Velocity & Temperature profiles with different values of Solutal Grashof number and Injection or Suction (*V*).

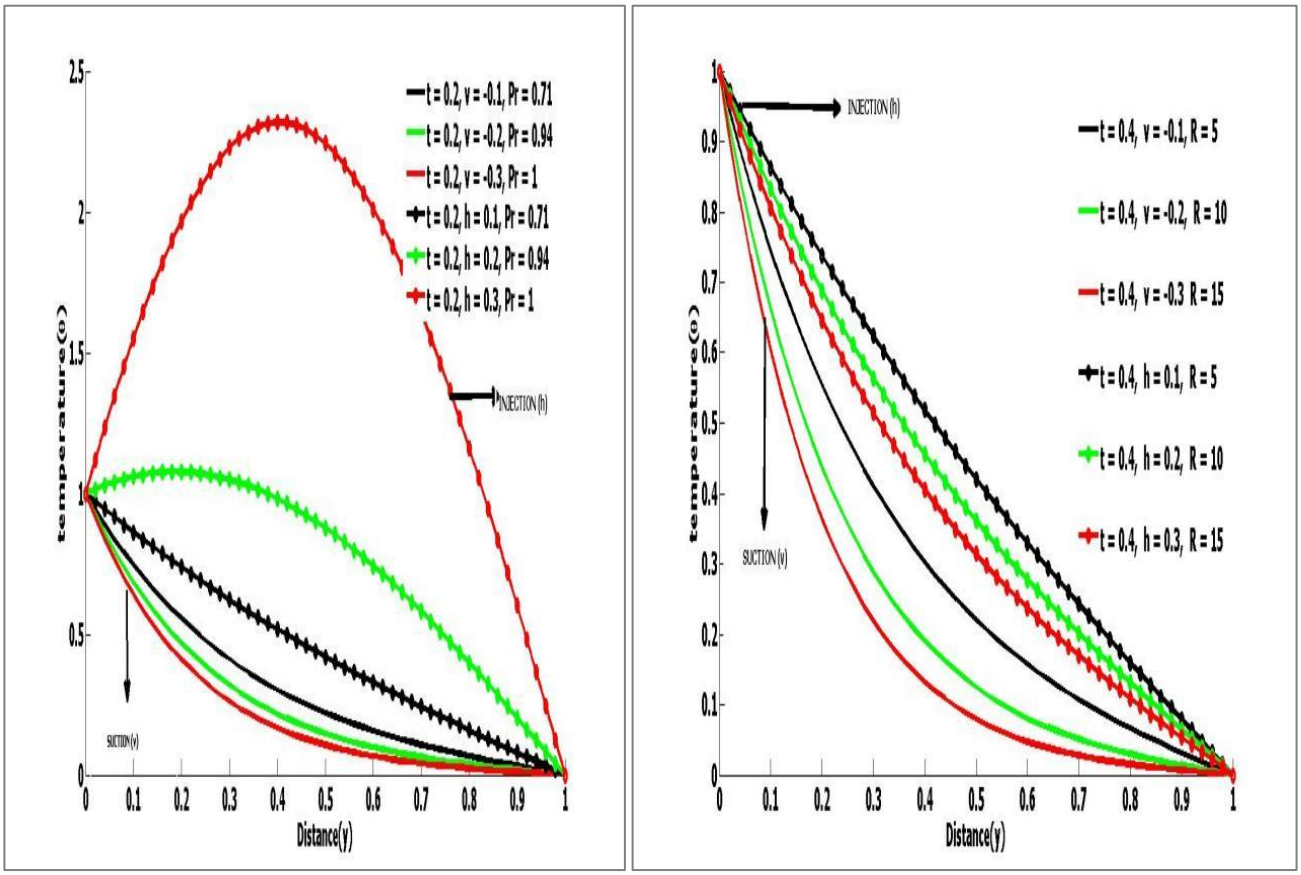

Figures 10 & 11: Temperature profiles with different values of prandtl number (Pr) and Radiation (R).

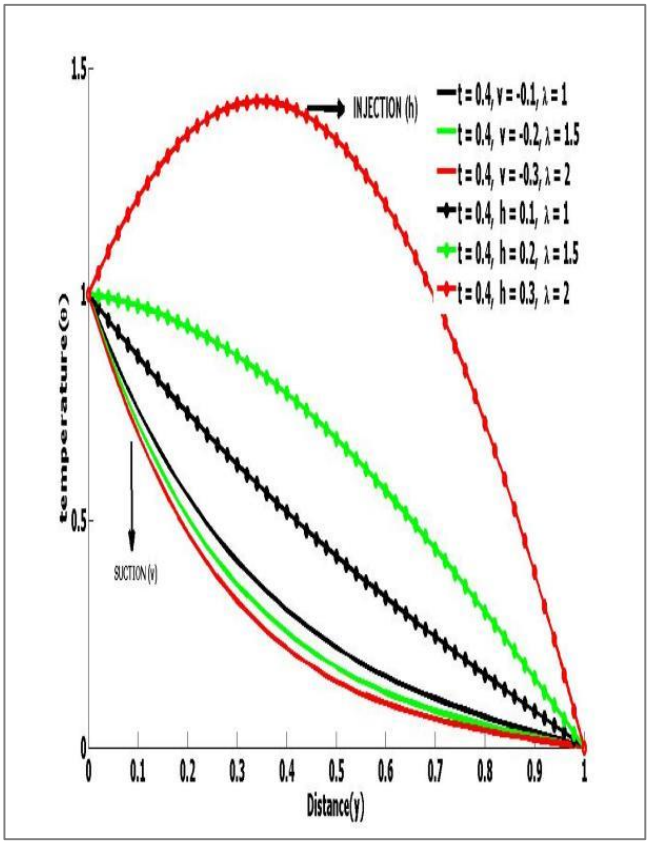

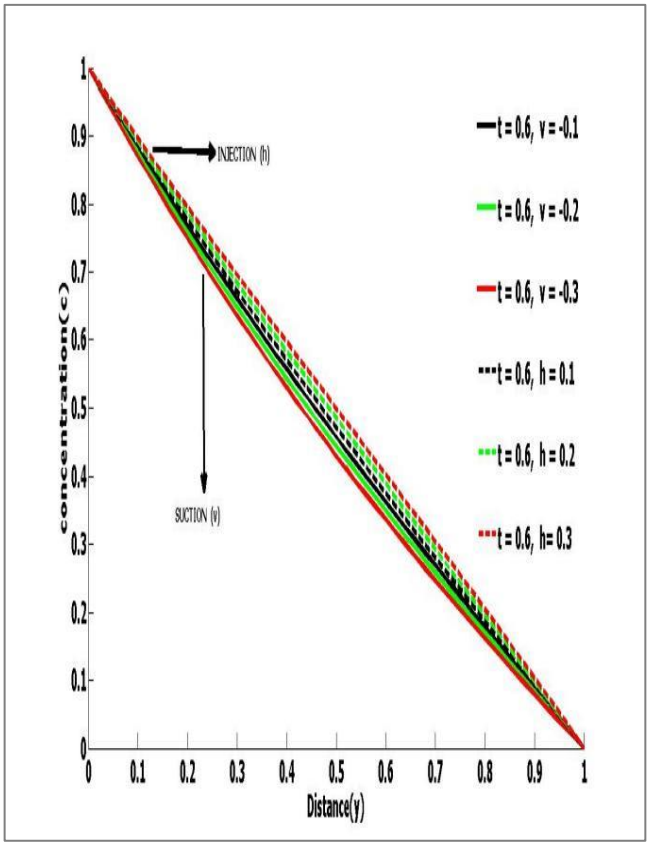

Figures 12 & 13: Temperature and Concentration profiles for different values of Variable thermal conductivity (λ) and Injection or Suction.

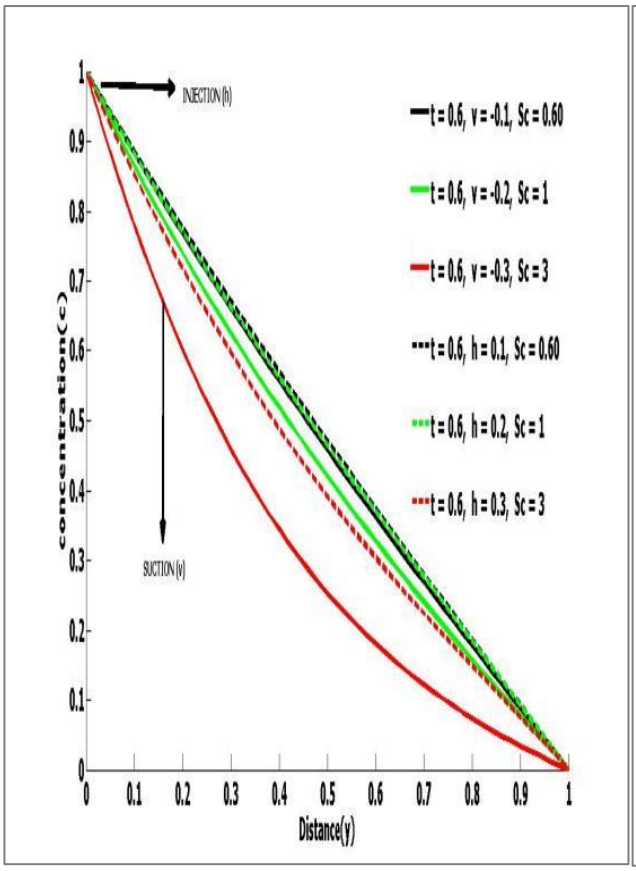

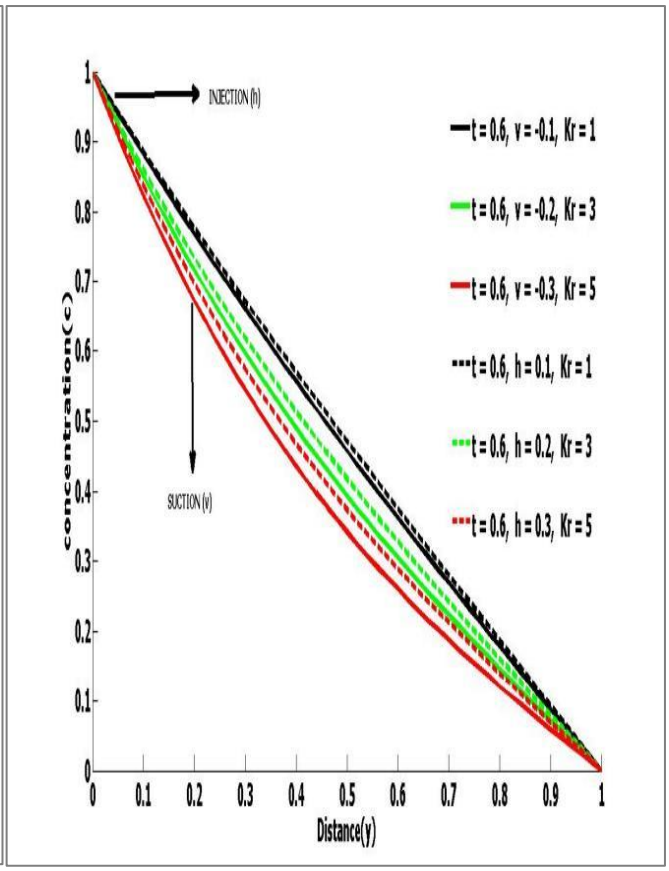

Figures 14 & 15: Concentration profiles for different values of Schmidt number (Sc) and Chemical reaction.

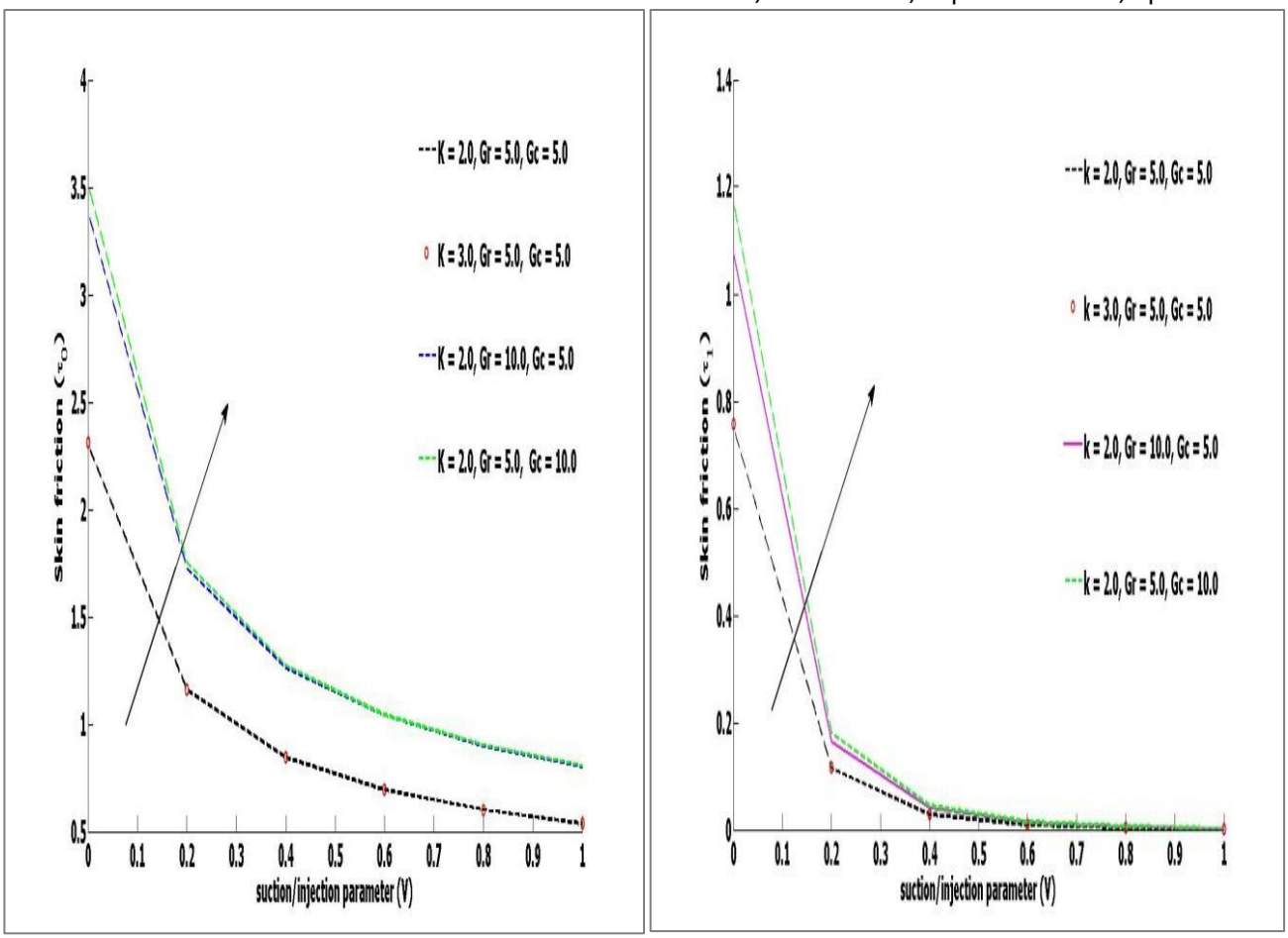

Figure 16 (a) & (b): Effect of suction/injection (V) on skin friction with k = 2.0, Gr = 5.0, Gc = 5.0, V = 0, 0.2, 0.4, 0.6, 0.8 & 1.

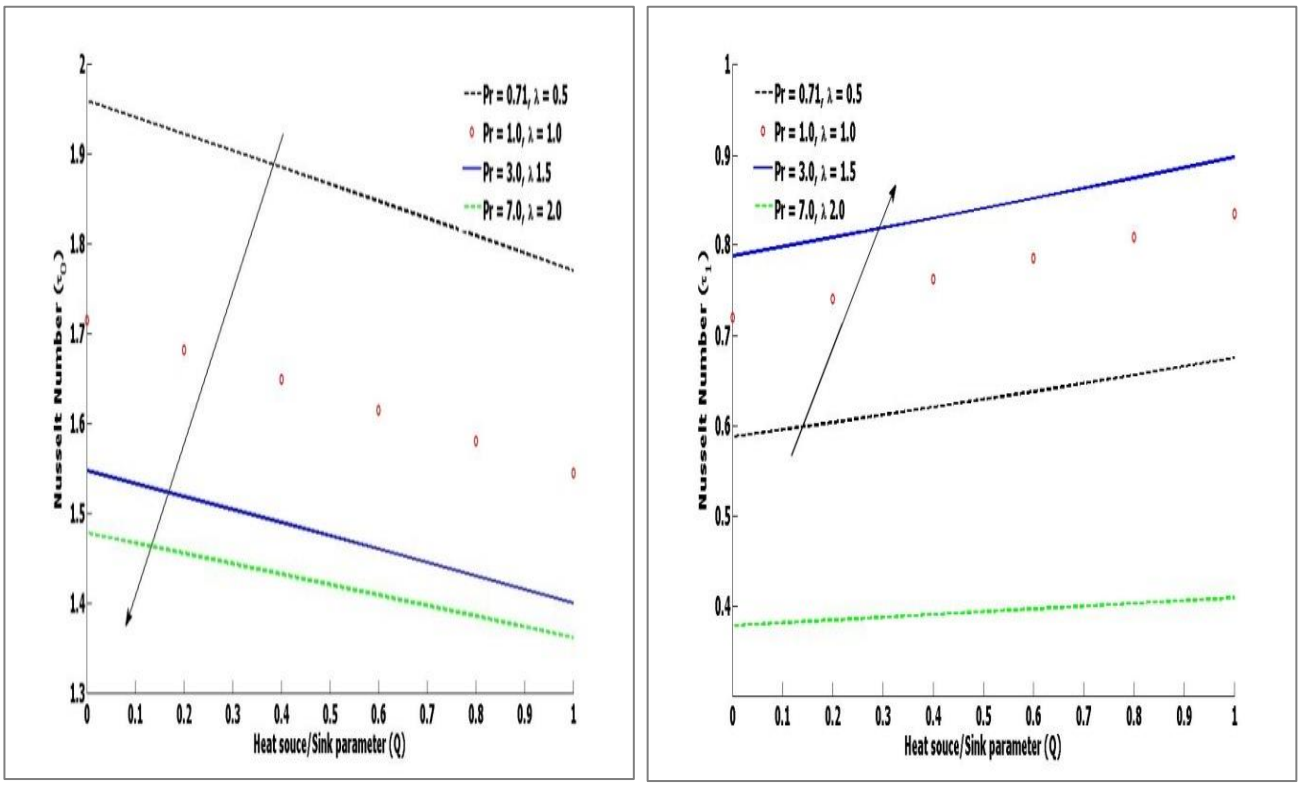

Figure 17 (a) & (b): Effect of Suction/injection (V) on nusselt number with Pr = 0.71, Lmd = 0.5, V = 0, 0.2, 0.4, 0.6, 0.8 &1.

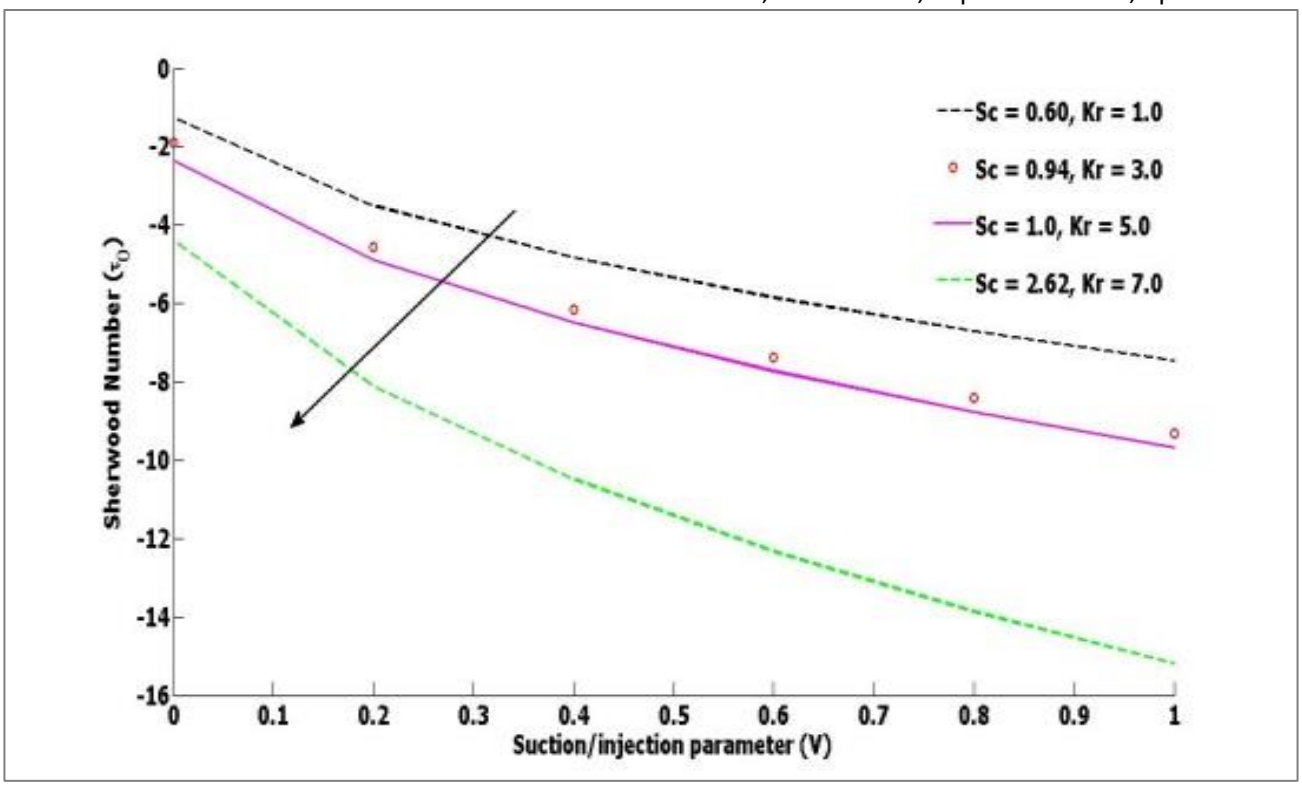

Figure 18: Effect of suction/injection (V) on Sherwood number with Sc = 0.60, Kr = 1.0, V = 0, 0.2, 0.4, 0.6, 0.8 & 1.

Figures 2 and 3 express the graphical representation of velocity profiles for the Anchor paper and Present work, respectively. Figure 2 agrees with the anchor paper, where the same flow behavior has been observed with a difference in enhancement of the velocity in the present work due to the presence of suction/injection.

The velocity profiles for different values of the parameters for suction/injection (V), magnetic field (M), and porous (k) are shown in Figures 4, 5, and 6. For all of the previously mentioned parameters, it is found that the velocity curve of the equivalent boundary layer thickness drops with rising suction values and increases with increasing injection values. This is because the fluid flow on the channel is controlled by the suction/injection parameter, which in turn affects the rate at which heat is transferred from the plate. The impact of Gr and Gc on the velocity profiles is depicted in Figures 6 and 7. It is evident that as Gr and Gc increase, so does the thickness of the momentum boundary layer. The boundary layer's thermal energy is the cause of this. Figure 8 illustrates how suction brings fluid at room temperature closer to the surface and thins the thermal boundary layer. In the case of injection, the same idea is applied, but in the reverse way. The influence of Prandtl number (Pr) over the temperature distributions is shown in Figure 9. The temperature of the fluid is found to decrease with increasing Prandtl number near the heated plate in terms of suction but increases near the cold plate in terms of injection. This causes the fluid's boundary layer thickness to rise, which in turn increases thermodynamics. The effects of the Radiation (R) Parameter on the temperature profile are seen in Figure 10.

The fluid temperature is radiated as particles in the boundary layer, which results in the decrease of the fluid by the increasing values of the Radiation (R) parameter both in terms of suction and injection. Figure 11 illustrates the effects of the Variable thermal conductivity (λ) parameter on the temperature distributions. It is seen that increasing values of Variable thermal (λ) increases the temperature of the fluid in case of injection and decreases in terms of suction. Figure 12 shows the effects of suction/injection on the concentration profiles. It is noticed that the concentration of the fluid increases with increasing values of injection and decreases with increasing suction. Figure. 13 displays the effects of the Schmidt number (Sc) parameter on the concentration distributions. It is observed that an increase in Schmidt number (Sc) corresponds to a weaker solute diffusivity, which allows a shallower penetration of the solutal effect. As a result the concentration decreases with increasing of Schmidt number (Sc). Figure 14 shows the effects of chemical reaction (Kr) on the concentration profile. It is noticed that increasing the values of chemical reaction parameters decreases the concentration profile both in terms of suction and injection. The logic is that as chemical reaction increases, the quantity of solute molecules undergoing them grows, which causes concentration to drop, which in turn reduces the likelihood of destructive chemical reactions.

Figure 16 (a) and (b) show the variation of skin friction profiles with respect to porous parameter (k), Thermal grashof number (Gr), Solutal grashof number (Gc), and Suction/injection (V) parameters. It is observed the skin friction coefficient rises with an increase in these parameters. Figure 17 (a) and (b) illustrate the graph of

Nusselt number. It is observed that Nusselt number decreases with increasing values of Prandtl number (Pr), Variable thermal conductivity (λ), and Suction/injection (V) parameters. Figure 18 demonstrates the graph of Sherwood number and noticed that Sherwood number deceases by the increasing of Schmidt number (Sc) and Chemical reaction (Kr) parameters.

CONCLUSION

"In view of the above findings highlighted the importance of considering suction/injection in designing systems for optimal heat and mass transfer which the anchor model lacked. Future research can be extended by incorporating the impact of viscous dissipation and heat source/sink to advance this present work and strengthen it".

ACKNOWLEDGEMENT

The authors extend their appreciation to tertiary education trust fund (TETFund) and Federal Polytechnic Kaura Namoda, Nigeria, for funding this research with the grant number as thus: TETF/DR&D/CE/POLY/KAURA NAMODA/IBR/2023/VOL.I.

APPENDIX

$p = \left(M + \frac{1}{k}\right)$, $\alpha = 1 + \lambda\theta$, $r_1 = \frac{\Delta t}{(\Delta y)^2}$, $r_2 = \frac{V\Delta t}{\Delta y}$, $r_3 = \frac{\Delta t}{Pr(\Delta y)^2}$, $r_4 = \frac{\Delta t\lambda}{\Delta y}$

$r_5 = \frac{\Delta t}{Sc(\Delta y)^2}$, $d_1 = r_1$, $d_2 = 1 + 2r_1$, $d_3 = 1 + r_2 - p\Delta t$, $d_4 = r_2$, $d_5 = \Delta t Gr$,

$d_6 = \Delta t Gc$, $d_7 = r_3\alpha$, $d_8 = 1 + 2r_3\alpha$, $d_9 = r_4$, $d_{10} = \left(1 + r_2 - \frac{\Delta t R}{Pr}()\right)$, $d_{11} = r_5$,

$d_{12} = 1 + 2r_5$, $d_{13} = 1 + r_2 - \Delta t Kr$, $d_{14} = r_2$.

NOMENCLATURE

C	Concentration
C_p	Specific heat at constant pressure
D	Mass diffusivity
G	Acceleration due to gravity
Gr	Thermal Grashof number
Gc	Solutal Grashof number
K	Porous parameter
Nu	Nusselt number
Pr	Prandtl number
Sc	Schmidt number
R	Radiation parameter
Kr	Chemical reaction parameter
T	Temperature
C_f	Skin friction
Sh	Sherwood number
u, v	Velocity in $x$direction and y -direction respectively
x, y	Cartesian coordinates along the plate and normal to it respectively
M	Magnetic field parameter
V	Suction/injection

GREEK LETTERS

β^*	Coefficient of expansion with concentration
β	Coefficient of thermal expansion
ρ	Density of fluid
σ_0	Stefan Boltzmann constant
λ	Variable thermal conductivity
σ	Electrical conductivity of the fluid
B_0	Magnetic field of constant strength

REFERENCES

Abiodun, O. A. and Kabir, T. M. (2020). The combine effect of variable viscosity and variable thermal conductivity on natural convection couette flow. *International Journal of thermo fluids*, 5-6. **[Crossref]**

Amos, S. I. Mojeed T. A. Abubakar, Jos U. and Bidemi. O. F. (2020). MHD free convective heat and mass transfer flow of dissipative casson fluid with variable. *Journal of Taibah University For Science*, 14(1), 851-862. **[Crossref]**

Babu, P. R. Rao, J. A. and Sheri, S. (2014). Radiation effect on MHD heat and mass transfer flow over a shrinking sheet with suction. *Jounal of applied fluid mechanics*, 7(4),641- 650. **[Crossref]**

Bhattacharya, K. (2011). Effects of radiation and heat source/sink on unsteady MHD boundary layer flow and heat transfer over a shrinking sheet with suction/injection. *Front. Chem. Sc. Eng.* 5(3), 376-384. **[Crossref]**

Hsiao, KL. (2010). Heat and mass transfer for Viscous flow with radiation effect past a non-linear stretching sheet. *World Academy of Science, Engineering and Technology*, 62,326-330.

Ishak, A. Merkin, J. H. Nazar, R. and Pop, I. (2008). " Mixed convection boundary layer flow over a permeable vertical surface with prescribed wall

heat flux," *ZAMP: Zeitschript fur angewandte Mathematik und hysik,* vol. 59, no.1, pp. 100-123. **[Crossref]**

Iranian. D. Sudarmozhi, K. Ilyas, Khan. and Abdullahi, Mohamed. (2023). Significance of heat generation and impact of suction/injection on Maxwell fluid over a horizontal plate by the influence of radiation. *International journal of Thermo fluids*, vol. 20, pp. 2666-2027. **[Crossref]**

Jha, B. K. Isah, B. Y. and Uwanta, I. J. (2016). Combined effect of suction/injection on MHD free – convection flow in a vertical channel with thermal radiation. *Ain Shams Engineering Journal*, 9: 1069-1088. **[Crossref]**

Jha. B.K. and Aina. B. (2018). Role of suction/injection on steady fully developed mixed convection flow in a vertical parallel plate micro channel. *Ain Shams Eng J* ,9: 747-755. **[Crossref]**

Jha. B.K. Luqman. A. and Michael, O.O. (2018). Unsteady hydromagnetic-free convection flow with suction/injection. *J Taibah Univ Sci* , 13: 136-145. **[Crossref]**

Kareem, R. A. and Salawu, S. O. (2017). Variable viscosity and thermal conductivity effect of soret and dufour on inclined magnetic field in Non-Darcy Permeable Medium with dissipation. *Journal of Mathematics and Computer Science*, 22(3), 1-12. **[Crossref]**

Lavanya, B. and Ratmann, A. L. (2014). Radiation and mass transfer effects on un steady MHD natural convective flow past a vertical porous plate embedded in a porous medium in a ship flow regime with the heat source / sink effect . *Int .J . Eng . Tech. Res.*2.

Majid, Hussain. Akhtar, Ali. Mustapha, Inc. Ndolane, Sene. and Muhammad, Hussan. (2022). Impacts of Chemical reaction and Suction/Injection on the Mixed Convective Williamson Fluid past a Penetrable Porous Wedge. *Journal of Mathematics,* vol.22. 10pages. **[Crossref]**

Parasad, K. Vaidia, H. Makinde, O. Vajravelu, K. and Valmiki, R. (2020). Studied the effect of suction/ injection and heat transfer on unsteady MHD flow over a stretchable rotating disk. *Latin American Applied Research* 50(3), 159-165. **[Crossref]**

Quader, A. and Alam, M. (2021). Soret and Duour Effects on unsteady Free Convection Fluid Flow in the Presence of Hall Current and Heat Flux. *Journal of Applied Mathematics and Physics,* 9, 1611-1638. **[Crossref]**

Rehman, S. Idrees, M. Shah. R. A. and Khan, Z. (2019). Suction/injection effects on an unsteady MHD Casson thin film flow with slip and uniform thickness over a stretching sheet along variable flow properties. 26,1-24. **[Crossref]**

Sarojamma, G. Vijiya, L. R. Satya, N. and Vajravelu, K. (2019). Variable thermal conductivity and thermal radiation effect on the motion of a micro polar fluid over an upper surface. *Journal of Applied and Computational Mechanics*, 5(2), 441-453.

Seddek, M. A. and Salema, F. A. (2007). investigated the effects of temperature dependent viscosity and thermal conductivity on unsteady MHD convective heat transfer past a semi- infinite vertical porous plate in the presence of suction and magnetic field parameter. *Computational Material Science*, 40(2), 186-192. **[Crossref]**

Shojaefard, M. H. Noorpoor, A. R. Avanesians, A. and Ghaffapour, M. (2005). Studied suction/injection to control fluid flow on the surface of subsonic aircraft. *American Journal of Applied Sciences,* vol. 20, pp. 1474-1480. **[Crossref]**

Sree, P. K. S. and Alam, Md. M. (2021). Effect of variable viscosity and thermal conductivity on MHD natural convection flow along a vertical flat plate. *Journal of Advances in Mathematics and Computer Science*, 36(3), 58-71. **[Crossref]**

Sumera, D. Kamel, S. Liaquat, A. L. Kaouther, G. Sami, U. K. Chemsedddine. M and Lioua, Ko. (2022). Effect of thermal stability of hybrid nanofluid with viscous dissipation and suction/injection applications: Dual branch framework. *Journal of the Indian Chemical Society*. vol. 99, pp. 1017-1035. **[Crossref]**

Usman Halima. M. S. Magami, M. Ibrahim and Omokhuale, E. (2017). Combined effects of magnetic field and chemical reaction on unsteady natural convective flow in a vertical porous channel. *Asian journal of mathematics and computer research, 29(2), issn: 2395-4213(p),* pp. 87-100.

Usman Halima. Tasi'u, Ahmad, Rufa'i. and Emmanuel, Omokhuale. (2022). Effects of suction/injection on free convective radiative flow in a vertical porous channel with mass transfer and chemical reaction. *Ijsgs, vol. 8(4). Pp:28-37.* **[Crossref]**

Uwanta I. J. and Hamza M .M. (2014). Effect of suction / injection on unsteady hydromagnetic convective flow of reactive viscous fluid between vertical porous plates with thermal diffusion . *Hindawi International Scholarly Research Notices*,1—14. **[Crossref]**

Uwanta I. J. and Usman Halima. (2014). Effect of variable thermal conductivity on heat and mass transfer flow over a vertical channel with magnetic field intensity. *Journal of Applied and Computational Mathematics.* 3(2),48-56.

Uwanta, I. J. and Usman, H. (2015). Finite difference solution of MHD free convective flow with constant suction and variable thermal conductivity in a Darcy- Forchheimer porous medium. *IOSR Journal of Mathematics*, 2(1), 42-58.